A&A 461, L13–L16 (2007)
DOI: 10.1051/0004-6361:20066552

Astronomy & Astrophysics

Letter to the Editor

The extra-mixing efficiency in very low metallicity RGB stars⋆

A. Recio-Blanco and P. de Laverny

Dpt. Cassiopée, Observatoire de la Côte d'Azur, CNRS/UMR 6202, BP 4229, 06304 Nice Cedex 4, France
e-mail: [arecio;laverny]@obs-nice.fr

Received 12 October 2006 / Accepted 6 November 2006

ABSTRACT

Aims. After the first dredge-up, low-mass Red Giant Branch (RGB) stars experience an extra-mixing episode that strongly affects the chemical abundances on their surface. This mixing occurs at the bump in the luminosity function. In this Letter we describe the efficiency of the extra-mixing in RGB stars found in very metal-poor globular clusters (GC).
Methods. The VLT/ISAAC spectra of twenty stars located between the bump and the tip of the RGB in four GCs with metallicities between [Fe/H] = −1.2 and −2.5 dex were collected. The carbon isotopic ratios on their surface were derived from the second overtone ($\Delta v = 2$) bands of the CO molecule at 2.3 μm with the spectral synthesis method.
Results. It is found that the carbon isotopic ratios of very metal-poor GC stars always reach the equilibrium value of the CNO cycle almost immediately above the bump in the luminosity function. No additional mixing episode at brighter luminosities and no variations with the clusters' metallicity were detected. The extra-mixing is therefore found to be very efficient in metal-poor low-mass RGB stars, in very good agreement with theoretical expectations.

Key words. stars: abundances – stars: evolution – stars: late-type – globular clusters: individual: general

1. Introduction

During their ascent of the Red Giant Branch (RGB), low-mass stars undergo mixing processes that bring freshly synthetised nuclides to their surface. In standard stellar evolution theory (Iben 1964), chemical changes in the surface are only expected to be caused by convective dilution during the first dredge-up (1DUP) occurring at the base of the RGB: the convective envelope deepens and enters regions already processed by the central H-burning phase, thereby altering the surface abundances. This process leads to a decrease in the carbon isotopic ratio (^{12}C/^{13}C) from the main sequence value (∼90 in the solar case) to post 1DUP values around 20−25 (Charbonnel 2003 or Denissenkov & Herwig 2004). In addition, the carbon abundance drops, while the nitrogen one increases. Oxygen and all heavier element abundances, however, would remain unchanged. According to the standard scenario, the surface abundances after the 1DUP remain unaltered, as the convective envelope slowly withdraws outward in mass during the final stages of the RGB evolution.

This canonical picture is, however, challenged by an increasing amount of observational data demonstrating its limited validity (see, for instance, Brown & Wallerstein 1989 and, more recently, Smith et al. 2000 and Gratton et al. 2000). In fact, in most of the field and globular cluster (GC) low-mass evolved stars, the observed conversion of ^{12}C to ^{13}C and ^{14}N greatly exceeds the levels expected from standard stellar models. More recently, Shetrone (2003) derived ^{12}C/^{13}C ratios in low-metallicity GC RGB stars ([Fe/H] > −1.2) and found very low values, almost reaching the near-equilibrium value of the CNO cycle (^{12}C/^{13}C ∼ 3.5). This very clear evidence requires a non canonical mixing (named *extra-mixing*) between the shell and the bottom of the convective envelope (see for instance Charbonnel 2003 and Weiss 2006). Most of the observations supporting this evolutionary scenario indicate that extra-mixing begins at the RGB luminosity-function bump. This bump appears when the narrow burning H-shell reaches the sharp chemical discontinuity in the H-distribution profile caused by the deep penetration of the convective envelope. A drop in the stellar luminosity then occurs, revealed by a bump in the RGB luminosity distribution. This bump, predicted by Iben (1968) and detected by King et al. (1985), occurs at brighter luminosities for more metal-poor GCs.

As already proposed by Charbonnel (1994, 1995), observations strongly suggest that prior to the bump, the mean molecular weight gradient created during the 1DUP acts as a barrier to any mixing below the convective envelope. After the bump, the gradient of molecular weight above the H-burning shell is much lower, allowing the extra-mixing to act. Now, the extra-mixing scenario is well admitted, but its exact physical nature and efficiency are still objects of debate (see, for instance, Palacios et al. 2006). Furthermore, the extra-mixing efficiency at very low metal content is still poorly known, as is its metallicity dependence. We therefore present here carbon isotopic ratios of RGB stars in GC ten times metal-poorer (down to [Fe/H] ∼ −2.5) than presented in Shetrone (2003). They were derived from low-resolution spectra around the second overtone bands of the CO molecule at 2.3 μm. The selection of the targets, the observations, and their reduction are presented in Sect. 2. Section 3 is devoted to the derivation of the ^{12}C/^{13}C ratios and, we discuss the extra-mixing efficiency in such metal-poor stars in Sect. 4.

2. Target selection and observations

We selected three GCs with [Fe/H] ratios about ten times lower than in previous works: NGC 6397, M 30 (NGC 7099),

⋆ Based on observations collected with the VLT/ISAAC instrument at Paranal Observatory, ESO (Chile) – Programme 75.D-0228A.

and M 15 (NGC 7078) with [Fe/H] = −2.1, −2.3, and −2.45 dex, respectively. For the purpose of a comparison with Shetrone (2003), we also selected M 4 (NGC 6121 with [Fe/H] = −1.2 dex). For all these clusters (see Table 1), we adopted the metallicity scale of Kraft & Ivans (2003). The observed K_s-magnitudes of the M 15 and M 4 bumps were taken from Cho & Lee (2002; Ferraro et al. 2000 and Valenti et al. 2004 report a consistent value for M 15). For M 30 and NGC 6397, we estimated their K_s-bump magnitude from the relation derived by Valenti et al. (2004), from the photometric systems transformation of Carpenter (2001), and from distance moduli and extinctions in the Harris catalogue (1996, see next section for more details). This relation was checked for a very good agreement with the observed K_s-bump magnitudes of M 15 and M 4. The adopted K_s-magnitudes of the GC bump are reported in Table 1. Typical uncertainties for M_K-bump magnitudes are ±0.1 mag (Valenti et al. 2004). Taking into account errors on distance moduli and extinctions, the total error for the calculated K_s-bump magnitudes is of the order of 0.15 mag. It is around 0.1 mag. for the observed ones (Cho & Lee 2002).

Target selection was based on the photometry by Rosenberg et al. (2000a) for M 4 and NGC 6397, Rosenberg et al. (2000b) for M 15, and Momany et al. (2004) for M 30. The colour−magnitude diagrams of each GC were used to select stars located between the bump (or slightly less luminous) up to the tip of the RGB. The observed stars are listed in Table 1 with the naming convention of their corresponding photometry. Some fainter targets of the sample were finally not included in this work due to an unclear identification of their CO bands. We also checked the radial velocity of each target, derived from the collected spectra, in order to confirm their GC membership.

The observations were collected during the nights July 25−27, 2005, with the ISAAC instrument on the VLT/ANTU (ESO, Chile). We used a slit width of 1″, leading to a spectral resolution of about 3000 over the domain 2.275−2.39 μm. Objects were observed at two positions along the slit to remove the sky contribution (nodding technique). In most of the cases, the slit orientation was chosen in order to observe two objects simultaneously. Their position on the slit and the nodding/jitter parameters were defined to avoid spectra overlap. The number of nodding cycles varied from 3 to 5 and the detector integration time from 3.5 to 300 s, depending on the star magnitude. The total exposure times (without overheads) ranged between one minute for the brightest stars at the tip of M 4 and NGC 6397, down to one hour for the faintest targets above the bump of M 30 and M 15.

To remove the lines of the Earth's atmosphere, several telluric standards were observed at the same airmass and with the same instrumental configuration as the science targets, soon before or after them. The selected standards were featureless hot OB spectral type stars. The spectra were reduced with the ISAAC pipeline offered by ESO, and standard IRAF procedures were used for spectra extraction. Each target spectrum was then divided by the spectrum of its corresponding telluric standard. In practice, several telluric spectra were tried in order to remove the telluric lines as fully as possible. Finally, the observed spectra were normalised as proposed by Shetrone (2003). We first compute a synthetic spectrum with parameters and chemical abundances (see Sect. 3) as close as possible to the observed one. Then, the residual of the division of the observed spectrum by the synthetic one is fitted by a low-order spline, which is then used to normalise the observed spectrum. This procedure was performed iteratively until the best synthetic spectrum was found.

3. Determination of the carbon isotopic ratios

The carbon isotopic ratios were derived with the spectral synthesis method. Theoretical spectra were computed with the turbospectrum code (Alvarez & Plez 1998, and further improvements by Plez). Model atmospheres were interpolated in a grid of new-generation MARCS models (Gustafsson et al. 2002, 2006). These models are in LTE, spherical geometry and with an enhancement of the α-elements typical of such low-metallic environments ([α/Fe] = +0.4). The CNO abundances of the Sun revised by Asplund et al. (2005) were adopted, and Solar abundances of other chemical species are from Grevesse & Sauval (1998). The adopted line list consists in atomic lines from the VALD database (Kupka et al. 1999) and in CO lines, including its different isotopes, from (Goorvitch & Chackerian 1994). Other molecular lines were found to be invisible in the studied domain at such low metallicities. Finally, synthetic spectra were broadened by convolution with a Gaussian to match the observed line widths. This line list was checked by fitting the high-resolution IR spectrum of Arcturus (Hinkle et al. 1995) with stellar parameters and abundances from Peterson et al. (1993). We found $^{12}C/^{13}C = 6 \pm 1$ for the Arcturus spectrum degraded to our adopted ISAAC resolution, in very good agreement with previous determinations published since Griffin (1974).

For each target star, the effective temperature was derived from the $(V - K)$ and $(J - K)$ colour indices and the Alonso scale (1999, 2001), using the transformation equations between the different photometric systems from Carpenter (2001) and Bessel & Brett (1988). The IR magnitudes are from the 2MASS catalogue by Skrutskie et al. (2006). We estimated the extinction in K from the GC foreground reddening reported by Harris (1996, revised in 2003) and from the relations given in Cardelli et al. (1989). For M 4, differential reddening was estimated from Cudworth & Reed (1990) but, in the effective temperature determination of its members, we favoured the estimate derived from the $(J - K)$ colour, as it is less affected by the reddening. The surface gravity was calculated from the estimated effective temperatures, distance moduli (Harris catalogue), and isochrones from Pietrinferni et al. (2004). Finally, we estimated the microturbulent velocity from the empirical relation for metal-poor giant stars derived by Pilachowski et al. (1996).

Then, the carbon isotopic ratio of the target stars was derived following a procedure very close to the one adopted by Shetrone (2003). The metal abundance of each star was assumed to be the same as the one of its parent cluster (in the Kraft & Ivans scale 2003; see Table 1), and the oxygen abundance was adjusted from the α-enhancement of these GCs. We then varied the carbon abundance to match the ^{12}CO(4−2) band at 2.35 μm. The $^{12}C/^{13}C$ ratio was finally determined by fitting the ^{13}CO(2−0) band at 2.345 μm. We recall that the observed continuum was corrected when necessary with the new synthetic spectra (see Sect. 2) until a stable solution was achieved. We found that these two CO bands give the most reliable solution. It was indeed impossible to remove the telluric contamination accurately enough around the other ^{13}CO band available at 2.37 μm. Finally, the adopted procedure was found to be insensitive to uncertainties in the stellar parameters, since both ^{12}CO and ^{13}CO features vary with them in a similar way. Furthermore, because the ^{12}CO band are not saturated in these very-low metallicity atmospheres, the uncertainty on the micro-turbulent velocity was found not to affect the results. Thus, once the ^{12}CO band is fitted by assuming a given carbon abundance (and other stellar parameters and chemical abundances), only the $^{12}C/^{13}C$ ratio can be varied to fit the ^{13}CO feature.

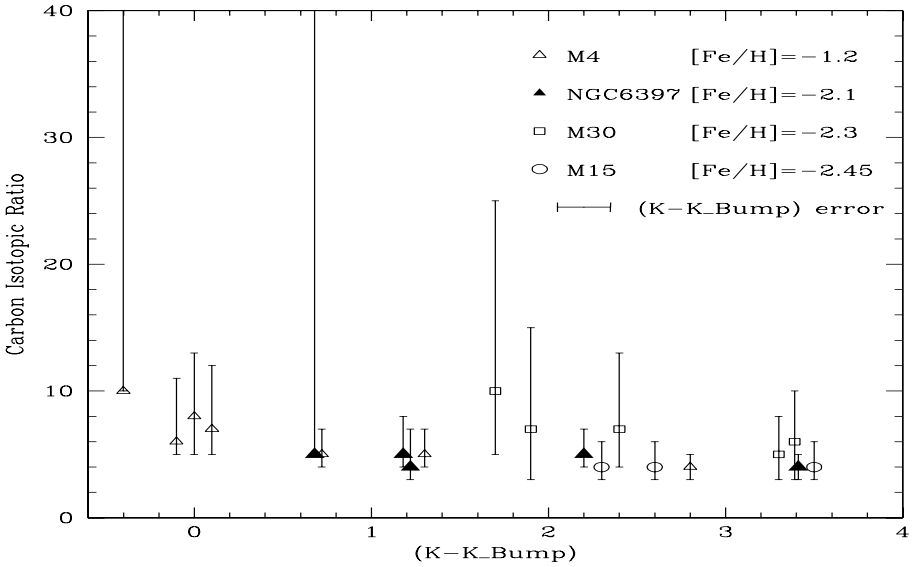

Fig. 1. Evolution of the carbon isotopic ratio with respect to the stellar K_s-magnitude above the bump in the RGB luminosity function of each globular cluster. The adopted K_s-bump magnitudes are reported in Table 1. The maximum error on $(K_s - K_s^{Bump})$ is shown in the upper right corner and, for a given cluster, the uncertainty on the relative stellar luminosities with respect to their bump is ±0.04 mag (see text for more details). The reported metallicity (in dex) of each GC is from Kraft & Ivans (2003). For two stars (one in M 4 and one in NGC 6397), we have only been able to derive lower limits for their carbon isotopic ratios. These limits are represented by a symbol located at the lower end of their error bar.

Table 1. Target properties and derived carbon isotopic ratios. The adopted metallicities (in dex) of each GC are in the Kraft & Ivans scale (2003). See text for references on V, K_s, and K_s^{Bump}-magnitudes and discussion of their errors.

Globular Cluster			Star	V	$(K_s - K_s^{Bump})$	$^{12}C/^{13}C$
Name	[Fe/H]	K_s^{Bump}				
M 4	–1.2	10.0	304	11.5	2.8	4^{+1}_{-1}
			113	12.5	1.3	5^{+2}_{-1}
			213	12.9	0.7	5^{+2}_{-1}
			456	13.5	0.1	7^{+5}_{-2}
			148	13.4	0.0	8^{+5}_{-3}
			53	13.5	-0.1	6^{+5}_{-1}
			152	13.7	-0.4	>10
NGC 6397	–2.1	9.7	1114	9.9	3.4	4^{+1}_{-1}
			224	10.7	2.2	5^{+2}_{-1}
			110	11.5	1.2	5^{+3}_{-1}
			429	11.5	1.2	4^{+3}_{-1}
			183	11.8	0.7	>5
M 30	–2.3	12.2	7917	12.1	3.4	6^{+4}_{-3}
			3998	12.1	3.3	5^{+3}_{-2}
			7640	12.6	2.4	7^{+6}_{-3}
			3711	13.0	1.9	7^{+8}_{-4}
			7927	13.2	1.7	10^{+15}_{-5}
M 15	–2.45	12.9	1662	12.8	3.5	4^{+2}_{-1}
			58	13.3	2.6	4^{+2}_{-1}
			665	13.5	2.3	4^{+2}_{-1}

The derived carbon isotopic ratios are given in Table 1. The corresponding errors are completely dominated by (i) the signal-to-noise ratio of the observed stellar and telluric spectra, (ii) the removal of the telluric absorptions, and (iii) the normalisation of the observed spectrum (these last two points being the dominant source of error). The error bars reported in Table 1 have been estimated by varying the $^{12}C/^{13}C$ ratio, taking all these uncertainties into account and, in particular, the continuum location around the ^{12}CO and ^{13}CO bands. For low $^{12}C/^{13}C$ values, errors are found to be much smaller due to the greater strength of the ^{13}CO band. For higher $^{12}C/^{13}C$, this band can be very weak, leading to much larger error bars.

4. Extra-mixing efficiency in very metal-poor stars

Figure 1 presents our derived carbon isotopic ratios with respect to the evolutionary status of the targets above the luminosity function bump. Comparing the stellar K_s-magnitude with the K_s-magnitude of the bump as in Fig. 1 has the advantage of avoiding uncertainties in distance moduli and interstellar absorptions. Moreover, for the case of M 4, this procedure diminishes any uncertainties due to diffential reddening. Errors in $(K_s - K_s^{Bump})$ are therefore dominated by the uncertainty on K_s^{Bump} and are close to ±0.15 mag in the worst cases (see Sect. 2). Of course, for a given cluster, the uncertainty on the relative positions of its members with respect to the bump luminosity is much fainter, since the 2MASS photometric error is about $\Delta K_s \simeq 0.04$ mag.

It can be seen that the carbon isotopic ratios are always found to be very low and close to or equal to the theoretical equilibrium value (within error bars), even immediately above the bump. In the case of NGC 6397 and M 15, the $^{12}C/^{13}C$ ratio is indeed found to always be smaller than 5 for a wide range of luminosities on the upper RGB, starting just above the bump. For M 30, slightly higher values (around 6 in average) are found, but they are still compatible with the CNO equilibrium value and the extra-mixing scenario. We therefore do not detect any variation with metallicity: the extra-mixing appears to be very efficient whatever the value of [Fe/H] is, leading to a large decrease in the carbon isotopic ratio down to the equilibrium value. Unfortunately, we were unable to derive carbon isotopic ratios of stars fainter than the bump for these very metal-poor GCs in order to precisely define where the extra-mixing starts and what its exact duration is. This would require much larger SNR spectra with higher spectral resolution. Finally, there is a group of three M 4 stars close to the bump but with rather low carbon isotopic ratios. These stars have therefore already experienced the extra-mixing episode, suggesting that the M 4 bump could be slightly fainter (by about 0.1 mag).

On the other hand, our determinations for M 4 stars can be compared to the work of Shetrone (2003). First of all, it can be seen that the carbon isotopic ratios in both studies are very similar. In addition, we observed two of the M 4 RGB stars studied by Shetrone: the star M 4#304 (named M 4#4511 by Shetrone) and the star M 4#456 (identified as M 4#4507 by him). For the first one, we measure $^{12}C/^{13}C = 4^{+1}_{-1}$, which is in very good

agreement within the error bars with Shetrone's $^{12}C/^{13}C = 5^{+2}_{-2}$ determination. In contrary, we derived $^{12}C/^{13}C = 7^{+5}_{-2}$ for M 4#456, whereas Shetrone found $^{12}C/^{13}C > 15$. We checked this discrepancy carefully and are fairly confident of our $^{12}C/^{13}C$ determination since (i) the SNR of our spectrum appears to be better than Shetrone's (see his Fig. 1) and (ii) M 4#456 is slightly more luminous than the bump, so that it should have already experienced the extra-mixing episode as confirmed by our rather low estimate of its carbon isotopic ratio. Nevertheless, the same star is slightly fainter than Shetrone's M 4 bump estimate. This disagreement could be explained by the uncertainties in the M 4 distance modulus, which is needed to calculate the absolute magnitude values that he uses. Finally, Shetrone proposes that a small decline with increasing luminosity (from just above the bump up to the tip) was present in his data, suggesting a continued mixing. The rather small statistics per individual GC, together with the reported uncertainties on $^{12}C/^{13}C$, do not allow us to confidently explore the existence of this trend.

Our conclusions can also be discussed with respect to the results of Gratton et al. (2000) who derived $^{12}C/^{13}C \sim 6^{+2}_{-1}$ up to 8^{+2}_{-2} in nine field upper-RGB stars with metallicity lower than -2 dex. Although some of their estimates agree with ours, others seem to be higher than the CNO cycle equilibrium value. This discrepancy could result from the uncertainty on the precise location of the onset of the extra-mixing episode (i.e. the bump for GC stars) for field stars. Indeed, the maximum inward penetration of the convective envelope occurs at higher luminosities for higher stellar masses or lower metallicity. In the Gratton et al. sample with stars with different masses and metallicities, this penetration therefore occurs at different luminosities. Thus, these RGB stars with slightly higher carbon isotopic ratios could still be experiencing their extra-mixing episode (in a GC, they would be found at or just above the bump).

Finally, it has to be pointed out that Carretta et al. (2005) were the first to report determinations of the carbon isotopic ratio in GC subgiant stars. They surprisingly found rather low $^{12}C/^{13}C$ ratios (mean value around 8) for these not very evolved stars that have still not experienced the 1DUP. They convincingly interpret their results by invoking the pollution of the analysed stars by previously evolved intermediate-mass AGB stars. If confirmed, this would reject the commonly admitted assumption that, before the bump, the carbon isotopic ratios in GC stars are still high. In consequence, the extra-mixing would not need to be as efficient as proposed by theoretical scenarios.

On the other hand, our derived carbon isotopic ratios for low-mass very metal poor RGB stars are in very good agreement with extra-mixing estimates. For instance, Charbonnel (1995; see also Denissenkov & Vandenberg 2003) proposes that rotation induced extra-mixing leads to a decrease of $^{12}C/^{13}C$ down to 3.5 for stars with 0.8 $M_\odot$ and $Z = 10^{-4}$ (i.e. close to the properties of our targets). In such low-metallicity stars, the mean molecular barrier, which inhibits the extra-mixing, would be much lower. That already leads to a very low $^{12}C/^{13}C$ ratio just above the bump luminosity as observed in our work. However, although the agreement appears very convincing, these models are based on a parametric approach. More physically realistic simulations of rotating low-mass stars have been performed recently by Palacios et al. (2006) and show that self-consistent models, where the rotational transport is treated within the stellar evolution code, lead to chemical variations that are too small at the stellar surface. Open questions therefore still remain in the modelling of rotating, evolved low-mass stars to reproduce the evolution of the observed chemical abundances on their surface.

In summary, we therefore confirm that the extra-mixing scenario is efficient in any stellar system: field stars (Gratton et al. 2000), low (Shetrone 2003), and very-low (this work) metallicity GC. Stars brighter than the RGB luminosity function bump already show the signatures of that mixing. Furthermore, within the uncertainties, the extra-mixing efficiency is found to be independent of the clusters metal content.

Acknowledgements. We thank the anonymous referee for constructive remarks. We acknowledge the MARCS collaboration for its continuous efforts in computing stellar atmosphere models. B. Plez is also thanked for providing molecular line lists and tools for computing stellar spectra. The VALD database was used when building the atomic lines. Y. Momany is acknowledged for his help on M 30 astrometry. A. Recio-Blanco thanks the European Space Agency for financial support through its post-doctoral fellowship programme. Many thanks to Magali and Benjamin for their careful reading of the manuscript!

References

Alonso, A., Arribas, S., & Martínez-Roger, C. 1999, A&AS, 140, 261
Alonso, A., Arribas, S., & Martínez-Roger, C. 2001, A&A, 376, 1039
Asplund, M., Grevesse, N., Sauval, A. J., et al. 2005, A&A, 431, 693
Alvarez, R., & Plez, B. 1998, A&A, 330, 1109
Bessel, M. S., & Brett, J. M. 1988, PASP, 100, 1134
Brown, J. A., & Wallerstein, G. 1989, AJ, 98, 1643
Cardelli, J. A., Clayton, G. C., & Mathis, J. S. 1989, ApJ, 345, 245
Carpenter, J. M. 2001, AJ, 121, 2851
Carretta, E., Gratton, R. G., Lucatello, S., et al. 2005, A&A, 433, 597
Charbonnel, C. 1994, A&A, 282, 811
Charbonnel, C. 1995, ApJ, 453, L41
Charbonnel, C. 2003, in CNO in the Universe, ed. Charbonnel-Schaerer, ASP Conf. Ser. 304, 303
Charbonnel, C., Brown, J. A., & Wallerstein, G. 1998, A&A, 332, 204
Cho, D.-H., & Lee, S.-G. 2002, AJ, 124, 977
Cudworth, K. M., & Rees, R. 1990, AJ, 99, 1491
Denissenkov, P. A., & VandenBerg, D. A. 2003, ApJ, 539, 509
Denissenkov, P. A., & Herwig, F. 2004, ApJ, 612, 1081
Ferraro, F. R., Montegriffo, P., Origlia, L., & Fusi Pecci, F. 2000, AJ, 119, 1282
Goorvitch, D., & Chackerian, C. 1994, ApJS, 91, 483
Gratton, R. G., Sneden, C., Carretta, E., et al. 2000, A&A, 354, 169
Grevesse, N., & Sauval, A. J. 1998, Space Sci. Rev., 85, 161
Griffin, R. 1974, MNRAS, 167, 645
Gustafsson, B., Edvardsson, B., Eriksson, K., et al. 2002, ASP Conf. Ser., 288, ed. I. Hubeny, D. Mihalas, & K. Werne, 331
Gustafsson, B., Edvardsson, B., Eriksson, K., et al. 2006, in preparation
Harris, W. E. 1996, AJ, 112, 1487
Hinkle, K., Wallace, L., & Livingston, W. 1995, PASP, 107, 1042.
Iben, I. Jr. 1964, ApJ, 140, 1631
Iben, I. Jr. 1968, Nature, 220, 143
King, C. R., Da Costa, G. S., & Demarque, P. 1985, ApJ, 299, 674
Kraft, R. P., & Ivans, I. I. 2003, PASP, 115, 143
Kupka, F., Piskunov, N. E., Ryabchikova, T. A., et al. 1999, A&AS, 138, 119
Momany, Y., Bedin, L. R., Cassisi, S., et al. 2004, A&A, 420, 605
Palacios, A., Charbonnel, C., Talon, S., et al. 2006, A&A, 453, 261
Peterson, R. C., Dalle Ore, C. M., & Kurucz, R. L. 1993, ApJ, 404, 333
Pietrinferni, A., Cassisi, S., Salaris, M., & Castelli, F. 2004, ApJ, 612, 168
Pilachowski, C. A., Sneden, C., & Kraft, R. P. 1996, AJ, 111, 1689
Rosenberg, A., Piotto, G., Saviane, I., & Aparicio, A. 2000a, A&AS, 144, 5
Rosenberg, A., Aparicio, A., Saviane, I., & Piotto, G. 2000b, A&AS, 145, 451
Shetrone, M. D. 2003, ApJ, 585, L45
Skrutskie, M. F., Cutri, R. M., & Stiening, R. 2006, AJ, 131, 1163
Smith, V. V., & Suntzeff, N. B. 1989, AJ, 97.1699
Smith, V. V., Hinkle, K. H., Cunha, K., et al. 2002, AJ, 124, 3241
Valenti, E., Ferraro, F. R., & Origlia, L. 2004, MNRAS, 354, 815
Weiss, A. 2006, in Chemical abundances and mixing in stars in the Milky Way and its satellites, 298, ESO astrophysics symposia, ed. Randich-Pasquini (Springer)